Available online at www.sciencedirect.com
SCIENCE DIRECT®
International Journal of Mass Spectrometry 240 (2005) 107–120
International Journal of Mass Spectrometry
www.elsevier.com/locate/ijms

Secondary ion mass spectrometry measurements of isotopic ratios: correction for time varying count rate

Kevin J. Coakley[a,*,1], David S. Simons[b], Andrew M. Leifer[a]

[a] *Statistical Engineering Division, National Institute of Standards and Technology, 325 Broadway, Boulder, C0 80305, USA*
[b] *Surface and Microanalysis Science Division, National Institute of Standards and Technology, Gaithersburg, MD, USA*

Received 21 August 2004; accepted 8 October 2004
Available online 19 November 2004

Abstract

In secondary ion mass spectrometry measurement systems, the count rate of isotopes may vary in time as a particle is consumed during the analysis. Since isotopes are measured sequentially, this drift can introduce systematic error into the estimate of the ratio of any two isotopes. We correct the measurements for drift by aligning the time series of isotopic pairs using a linear interpolation approach. We estimate an isotopic ratio for each of two cases. In one case the time series of the more abundant isotope is aligned with respect to the time series of the less abundant isotope. In the second case the less abundant isotope is aligned with respect to the more abundant one. We average both of these estimates to get a drift-corrected estimate. We present an analytical formula for the random uncertainty of the isotopic ratio that accounts for correlation introduced by interpolation. We also present an approximate hypothesis test procedure to detect and quantify possible temporal variation of the measured isotopic ratio during a single analysis. In a Monte Carlo study, the performance of the methods is quantified based on analysis of simulated data with complexity similar to that of real data generated by a secondary ion mass spectrometer.

Keywords: Drift correction; Isotopic ratio; Interpolation; Secondary ion mass spectrometry; Temporal variation; Uncertainty analysis

1. Introduction

Secondary ion mass spectrometry (SIMS) is a specialized analytical method that can be used to perform localized isotopic ratio measurements on a micrometer scale. Such measurements have broad applicability in areas of geology, astronomy, and biology [1]. A specific application area of recent interest is nuclear forensics, whereby SIMS has been applied to the search for evidence of uranium enrichment activities through the measurements of the relative abundances of U-235 and U-238 in micrometer-sized particles [2–6]. In SIMS measurement systems, the count rate of isotopes may vary in time as a particle is consumed during the analysis. Since only one isotope at a time is measured in conventional ion counting systems, this drift can introduce systematic error into the estimate of the ratio of any two isotopes. Hence, correcting the SIMS instrument for drift is critical to the accurate determination of isotopic ratios and their associated random uncertainties. Although chemical elements often have more than two isotopes, we consider their measurements here in a pairwise fashion, with the more abundant isotope of the pair designated as the major isotope and the less abundant one as the minor isotope.

In each of two interpolation schemes, we align one isotope time series with respect to the other. In the major–minor interpolation scheme, the minor time series is fixed and the major time series is interpolated. In the minor–major interpolation scheme, the major time series is fixed and the minor time series is interpolated. In simulation studies, we show that the average of the estimates obtained from both interpolation schemes is superior to the estimate computed either from the unaligned data or from a single interpo-

* Corresponding author. Tel.: +1 303 497 3895; fax: +1 303 497 3012.
[1] Contributions of NIST staff to this work are not subject to copyright laws in the US.
E-mail addresses: kevin.coakley@nist.gov (K.J. Coakley), david.simons@nist.gov (D.S. Simons), andrew.leifer@nist.gov (A.M. Leifer).

1387-3806/$ – see front matter © 2004 Elsevier B.V. All rights reserved.
doi:10.1016/j.ijms.2004.10.008

lation scheme for the case where the count rate varies in time.

We present a formula for the approximate standard deviation of the isotopic ratio estimated from the aligned data. Our formula accounts for the effect of interpolation on the variability of the data. We also present an approximate hypothesis test procedure to detect and quantify possible systematic temporal variation in the isotopic ratio time series data. Our new test is related to tests for spatial variation of isotopic ratio estimates computed from spatial data [7]. However, these methods were not originally designed for the case where SIMS data are interpolated in time.

In this work, we neglect other systematic errors such as dead time effects [8,9], mass bias effects and background contamination. Accounting for these effects in our estimation procedure and uncertainty analysis is straightforward but a subject beyond the scope of this work.

The concept of correcting mass spectrometric time series data for the effects of drift by a linear interpolation method is certainly not new. The novel contributions of this work include: (1) a rigorous statistical treatment of the uncertainty of the estimated isotopic ratio computed from the drift-corrected time series; (2) a method to reduce the systematic error of the isotopic ratio estimate computed from the interpolated data by averaging estimates computed from two different interpolation schemes; and (3) development of statistical methods to detect and quantify either systematic error or additional random variability (beyond counting statistics variability) in the isotopic ratio time series.

In Section 2, we comment on some mathematical difficulties associated with the expected value of the ratio of Poisson random variables. In Section 3, we present a measurement model for the data. In Section 4, we develop our alignment methods and an approximate formula for the random uncertainty of the isotopic ratio computed from the drift-corrected data. In Section 5, we develop a hypothesis test approach to detect possible temporal variation in the isotopic ratio of a particle. In Sections 6 and 7, we quantify the performance of our methods for simulated data with complexity typical of experimental data collected at NIST and remark on the limitations of our methods. In Section 8, we briefly discuss a suggested method to quantify possible systematic errors in the data for cases where we know that the isotopic ratio is stable in time. We also discuss a method to quantify the effect of unaccounted extra random variability on our estimate of the isotopic ratio.

2. Preliminary remarks

In this work, we present a method to reduce the systematic error, i.e., bias, of isotopic ratio estimates due to systematic temporal variation of the signals. The bias of a parameter estimate is the difference between its expected value and the true value of the parameter. Consider the estimate $\hat{r} = M/N$, where M and N are independent realizations (ion count measurements) of Poisson processes with expected values $r\lambda$ and λ. Since the probability that $N = 0$ is nonzero, the expected value of $\hat{r}$ is infinite. In order to construct an estimate with finite bias, we restrict attention to realizations of the data where the observed denominator term is positive. In effect, this means that the experimenter would ignore data where $N = 0$. For most experiments, λ is large and $P(N = 0) = \exp(-\lambda)$ is negligible. Thus, this restriction has no practical consequence on data acquisition in typical experiments of interest.

The conditional probability of observing a particular positive realization of N is

$$P(N|N > 0) = \frac{1}{1 - \exp(-\lambda)} \frac{\exp(-\lambda)\lambda^N}{N!}. \tag{1}$$

One can show that the expected value of the inverse of the positive realizations of N is

$$E\left(\frac{1}{N}|N > 0\right) \approx \frac{1}{\lambda}\left(1 + \frac{1}{\lambda}\right). \tag{2}$$

Suppose that M is a realization of a Poisson process with expected value $r\lambda$. If M and N are independent, it follows that

$$E\left(\frac{M}{N}|N > 0\right) = E(M|N > 0)E\left(\frac{1}{N}|N > 0\right) \approx r\left(1 + \frac{1}{\lambda}\right). \tag{3}$$

For more discussion about the expected values of ratios of random variables, see [10, p. 180].

Our analysis demonstrates that the expected value of the measured isotopic ratio computed for data in the restricted sample space is finite. Moreover, the fractional bias of the estimate $\hat{r} = M/N$ is approximately $1/E(N)$.

3. Measurement model

We assume that minor and major isotope counts are observed in an alternating scheme. The kth, where $k = 1, \ldots, K$, minor isotope measurement is made over a counting time interval centered at $t_m(k)$. The kth major isotope is measured over a counting time interval centered at $t_n(k)$. The widths of the minor and major intervals (bins) are respectively Δ_m and Δ_n. We denote the measured major and minor isotope counts for the kth cycle of the experiment as $n(k)$ and $m(k)$. We assume that the observed quantities $m(k)$ and $n(k)$ are realizations of Poisson processes with expected values

$$E(m(k)) = \int_{t_m(k)-\Delta_m/2}^{t_m(k)+\Delta_m/2} \lambda_m(t)\,\mathrm{d}t \tag{4}$$

and

$$E(n(k)) = \int_{t_n(k)-\Delta_n/2}^{t_n(k)+\Delta_n/2} \lambda_n(t)\,\mathrm{d}t, \tag{5}$$

where the count rates $\lambda_m(t)$ and $\lambda_n(t)$ may vary in time. In this work, we assume that $m(k)$ and $n(k)$ are independent random variables. Thus, the fluctuations $m(k) - E(m(k))$ and $n(k) - E(n(k))$ are uncorrelated even though $E(m(k))$ and $E(n(k))$ are dependent.

For stable count rates, a natural estimate for the isotopic ratio r is

$$\hat{r} = \frac{\Delta_n}{\Delta_m} \frac{\sum_{k=1}^{K} m(k)}{\sum_{k=1}^{K} n(k)}. \tag{6}$$

For the case where the count rates vary in time, the above estimate may be biased because the measurements of the corresponding minor and major isotope counts do not occur at the same time.

4. Alignment

In one linear interpolation scheme, we predict the number of major counts that would have been observed had $t_n(k)$ equaled $t_m(k)$. That is, we align the major isotope time series with respect to the minor isotope time series. In the other linear interpolation scheme, we predict the number of minor counts that would have been observed had $t_m(k)$ equaled $t_n(k)$. Because the actual count rate may not be exactly a linear function of time, each estimate is biased. In general, for the cases studied here, the two interpolation schemes produce estimates with biases of comparable magnitude but different sign. Thus, we average the two estimates to reduce bias. We will demonstrate that the isotopic ratio estimates produced by each of the interpolation schemes have similar standard deviations. Because the two estimates are highly correlated, the standard deviation of the average of the estimates is nearly the same as the standard deviation of either estimate.

In either linear interpolation scheme, we predict the observed number of counts for an interval where no data was taken by taking a weighted average of the observed counts from the two nearest intervals where data was taken. For the special case where the count rate varies linearly with time, the systematic error associated with either linear interpolation scheme vanishes because the expected value of the predicted number of counts for any interval equals the expected value of what would have been observed for that interval had data been taken. In general, the accuracy of either interpolation scheme depends on the validity of the assumption that the count rate can be approximated as a linear function of time in the immediate neighborhood that includes the interval of interest and the two nearest intervals. The validity of our method does not depend on whether the count rate is monotonically increasing or decreasing in any time interval of interest. For the general case where the count rate is a nonlinear function of time but approximately linear over contiguous time intervals where data is taken, we expect our method to work well. One can construct cases where our method is not expected to work well. For instance, our averaging method will not compensate for systematic error due to a periodically varying count rate (with a large amplitude) when the frequency of the sinusoidal variation equals the data sampling rate.

4.1. Alignment: major to minor

Without loss of generality, we assume that the minor isotope is measured first. We define the predicted number of major counts corresponding to a time with the same center as the kth minor isotope measurement as $\hat{n}(k)$. After alignment, we get a series of isotope count pairs $(m(k), \hat{n}(k))$, where $k = 2, \ldots, K$. A linear interpolation approach yields

$$\hat{n}(k) = \alpha_n(k) n(k-1) + \beta_n(k) n(k) \tag{7}$$

where

$$\alpha_n(k) = \frac{t_n(k) - t_m(k)}{t_n(k) - t_n(k-1)} \tag{8}$$

and

$$\beta_n(k) = \frac{t_m(k) - t_n(k-1)}{t_n(k) - t_n(k-1)}. \tag{9}$$

For this interpolation scheme, the estimated value of the isotopic ratio is

$$\hat{r} = \frac{M}{\hat{N}} \frac{\Delta_n}{\Delta_m}, \tag{10}$$

where

$$M = \sum_{k=2}^{K} m(k), \tag{11}$$

and

$$\hat{N} = \sum_{k=2}^{K} \hat{n}(k). \tag{12}$$

Based on a propagation-of-error method (Appendix A) similar to the one described in [7], we estimate the variance of $\hat{r}$ as

$$\widehat{\mathrm{VAR}}(\hat{r}) = \left(\frac{\Delta_n}{\Delta_m \hat{N}}\right)^2 \left[\widehat{\mathrm{VAR}}(M)(1 + \hat{N}^{-2}\widehat{\mathrm{VAR}}(\hat{N})) + \left(\frac{\Delta_m \hat{r}}{\Delta_n}\right)^2 \widehat{\mathrm{VAR}}(\hat{N})\right]. \tag{13}$$

Based on the assumption that the observed counts are Poisson random variables, we approximate the variance of M as

$$\widehat{\mathrm{VAR}}(M) = \sum_{k=2}^{K} m(k). \tag{14}$$

From Eqs. (7) and (12), we have that

$$\hat{N} = \sum_{k=1}^{K} \gamma_n(k) n(k), \tag{15}$$

where $\gamma_n(1) = \alpha_n(2)$, $\gamma_n(K) = \beta_n(K)$, and $\gamma_n(k) = \alpha_n(k+1) + \beta_n(k)$ for $1 < k < K$. If x and y are independent random variables and a and b are constants, $\mathrm{VAR}(ax + by) = a^2\mathrm{VAR}(x) + b^2\mathrm{VAR}(y)$. Hence, we approximate the variance of $\hat{N}$ as

$$\widehat{\mathrm{VAR}}(\hat{N}) = \sum_{k=1}^{K} \gamma_n^2(k) n(k). \tag{16}$$

4.2. Alignment: minor to major

The theoretical development for the alternative alignment scheme, where we align the minor isotope time series with respect to the major isotope time series, is similar to the above. For the minor–major interpolation scheme,

$$\hat{r} = \frac{\hat{M}}{N}\frac{\Delta_n}{\Delta_m} \tag{17}$$

and

$$\widehat{\mathrm{VAR}}(\hat{r}) = \left(\frac{\Delta_n}{\Delta_m N}\right)^2 \left[\widehat{\mathrm{VAR}}(\hat{M})(1 + N^{-2}\widehat{\mathrm{VAR}}(N)) + \left(\frac{\Delta_m \hat{r}}{\Delta_n}\right)^2 \widehat{\mathrm{VAR}}(N)\right], \tag{18}$$

where

$$N = \sum_{k=1}^{K-1} n(k) \tag{19}$$

and

$$\hat{M} = \sum_{k=1}^{K-1} \hat{m}(k). \tag{20}$$

The kth interpolated minor count value is

$$\hat{m}(k) = \alpha_m(k) m(k) + \beta_m(k) m(k+1), \tag{21}$$

where

$$\alpha_m(k) = \frac{t_m(k+1) - t_n(k)}{t_m(k+1) - t_m(k)} \tag{22}$$

and

$$\beta_m(k) = \frac{t_n(k) - t_m(k)}{t_m(k+1) - t_m(k)}. \tag{23}$$

We approximate the variances of N and $\hat{M}$ as

$$\widehat{\mathrm{VAR}}(N) = \sum_{k=1}^{K-1} n(k) \tag{24}$$

and

$$\widehat{\mathrm{VAR}}(\hat{M}) = \sum_{k=1}^{K} \gamma_m^2(k) m(k), \tag{25}$$

where $\gamma_m(1) = \alpha_m(1)$, $\gamma_m(K) = \beta_m(K-1)$, and $\gamma_m(k) = \alpha_m(k) + \beta_m(k-1)$ for $1 < k < K$.

If either M or $\hat{M}$ is 0, Eq. (13) or (18) predicts that $\widehat{\mathrm{VAR}}(\hat{r}) = 0$. Thus, for low count situations where the observed value of M or $\hat{M}$ is 0, our methods are not appropriate. The study of such 0 count cases is a topic for further study. In all cases studied here, the estimated isotopic ratio is nonzero.

5. Hypothesis test for temporal variation

We develop a hypothesis test to detect possible systematic temporal variation of isotopic ratio measurements for the major–minor interpolation scheme. The null hypothesis is that the isotopic ratio is constant in time and that the random variation of the data is due to Poisson counting statistics. As a caveat, it is possible that our test could detect systematic variation in the data unrelated to the temporal variation of the true isotopic ratio. Possible sources of such extra variation include imperfections of interpolation algorithms and random detector calibration errors or other instrumental instabilities that are not accounted for here. For cases where background signals are significant, systematic errors due to imperfect methods for background correction could also be difficult to distinguish from temporal variation of the true isotopic ratio. In [7], we quantified the systematic spatial variation of the isotopic ratio for cases where the evidence, based on the test statistic value, for such variation was strong. In Section 8, we offer guidance on how to modify the approach in [7] for the problem studied here.

Our goodness-of-fit statistic, χ_r^2, measures the difference between the ratio estimated for each cycle and the ratio estimated from all pooled data. The basic idea is to divide this difference by an approximation for the standard deviation of this difference. The sum of the squared standardized residuals is

$$\chi_r^2 = \sum_{k=2}^{K} \frac{(\hat{r}(k) - \hat{r})^2}{\widehat{\mathrm{VAR}}(\hat{r}(k))}, \tag{26}$$

where the estimated ratio for each cycle is

$$\hat{r}(k) = \frac{m(k)}{\hat{n}(k)}\frac{\Delta_n}{\Delta_m}, \tag{27}$$

and the estimate from the pooled data $\hat{r}$ is computed using Eq. (10). Using the same methodology as in the previous section, we approximate the variance of $\hat{r}(k)$ using a standard propagation-of-error approach as

$$\widehat{\mathrm{VAR}}(\hat{r}(k)) = \left(\frac{\Delta_n}{\Delta_m \hat{n}(k)}\right)^2 \left[\widehat{\mathrm{VAR}}(m(k)) \times (1 + \hat{n}^{-2}(k)\widehat{\mathrm{VAR}}(\hat{n}(k))) + \left(\frac{\Delta_m \hat{r}}{\Delta_n}\right)^2 \widehat{\mathrm{VAR}}(\hat{n}(k))\right]. \tag{28}$$

Based on Eq. (7), we approximate the variance of the kth interpolated major count and the kth observed minor count as

$$\widehat{\mathrm{VAR}}(\hat{n}(k)) = \alpha_n^2(k)n(k-1) + \beta_n^2(k)n(k), \tag{29}$$

where

$$\widehat{\mathrm{VAR}}(m(k)) = \frac{\Delta_m \hat{r}}{\Delta_n}\hat{n}(k). \tag{30}$$

Assuming that the $K-1$ terms $\hat{r}(k) = m(k)/\hat{n}(k)$ are independent Gaussian (normal) random variables, and the Eq. (28) variance approximation is exact, the test statistic χ_r^2 would have a chi-squared distribution with $K-2$ degrees of freedom. The sum of M independent Gaussian random variables (each with expected value 0) has a chi-squared distribution with M degrees of freedom. Our test statistic is assumed to have $K-2$ degrees of freedom rather than $K-1$ degrees of freedom because we use an estimate of r in the numerator terms in Eq. (26). In general, the degrees of freedom of goodness-of-fit statistics computed from K independent observations where the model has j adjustable parameters is $K-j$.

If the null hypothesis is true, then all random variability in the data is due to Poisson counting statistics. Suppose that we compute a particular value of χ_r^2 from a data set. The p-value for a given data set is $\int_{\chi_r^2}^{\infty} f(x)\,\mathrm{d}x$, where $f(x)$ is the probability density function (pdf) of the test statistic when the null hypothesis is true. In our work, we assume that $f(x)$ is the pdf for a chi-squared distribution with $K-2$ degrees of freedom. A very small p-value, say less than 0.05, is strong evidence for rejecting the null hypothesis. In some cases, researchers reject the null hypothesis only if the test statistic exceeds a selected critical value. To construct a test with nominal size κ, we chose a critical value such that the null hypothesis is rejected with probability κ. For our case, the critical level for a test with nominal size (false detection rate) 0.05 corresponds to the 0.95 quantile, i.e., 95th percentile, of a chi-squared distribution with $K-2$ degrees of freedom.

To illustrate our approach, we estimate false detection rates for the case where the major and minor count time intervals are both 1 s, and both the major and minor count rates are 1000 Hz. Thus, $r=1$. The midpoints of the count time intervals are such that $\alpha(k) = \beta(k) = 0.5$ (Eqs. (8) and (9)) for all k. We simulate $K=20$ pairs of unaligned $(m(k), n(k))$. For tests with nominal size 0.05 and 0.1, the corresponding approximate 68% confidence intervals for the observed rejection rates of the test are 0.04955 ± 0.0015 and 0.0977 ± 0.0021. In Fig. 1, we plot the rejection rates for a similar simulation study where $K=20$ as before, $r=0.01$, and the count rate of the minor isotope varies from 1 to 100 Hz. From this study, we conclude that our hypothesis test is approximate and may break down when the number of observed minor counts is very small.

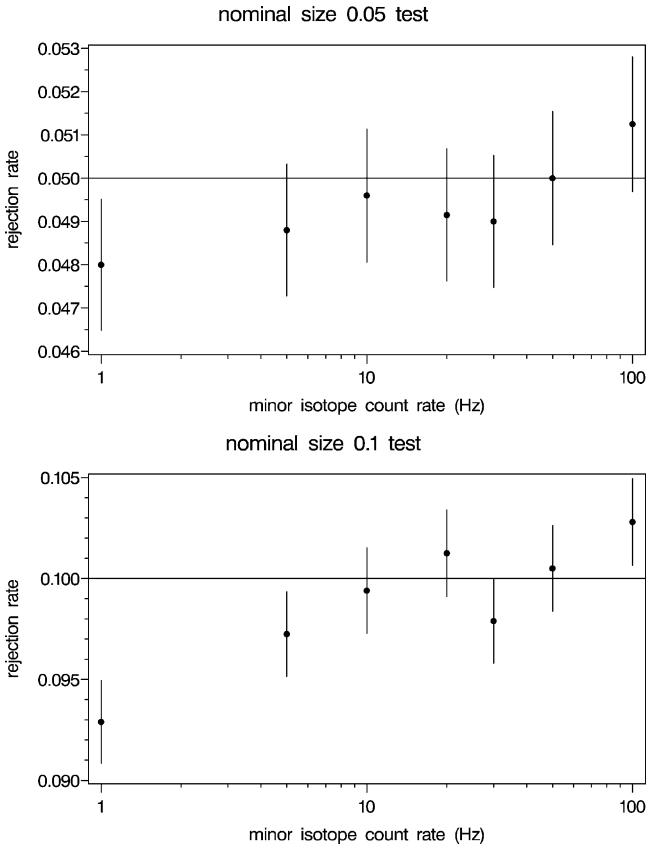

Fig. 1. Estimated rejection rate of hypothesis tests for case where $r=0.01$ and the count rates are stable in time. The number of simulated pairs of unaligned minor–major counts is $K=20$.

6. Example: real data

We analyze 50 cycles of SIMS measurements of boron isotopes B10 and B11 from a minute quantity of boron salt (Fig. 2). The isotopic ratio B10/B11 estimate from the raw data pairs, uncorrected for instrumental mass bias, is 0.27594, whereas the two interpolation schemes yield estimates of 0.27202 ± 0.00028 (major interpolated) 0.27216 ± 0.00028 (minor interpolated). In this work, $\hat{x} \pm \sigma$ corresponds to an approximate 68% confidence interval, i.e., a ± 1-sigma interval. The average of these two estimates, 0.27209, is plotted as a reference line in Fig. 3. The test statistic χ_r^2 and p-value for the hypothesis test for temporal variation are 47.238 and 0.504. Since the p-value is large compared to 0.05, we conclude that Poisson counting statistical variability explains the observed cycle to cycle variability in the data.

In Appendix B, we list software codes that implement our methods. The codes are written in the language R [11] which is a public domain software package that can be downloaded. In this work and in the codes, we assume that the minor isotope is measured first. If the major isotope is measured first, the codes can be run without modification if each isotopic time series is reversed. That is, transform the time midpoints from $t_1, t_2, \ldots, t_K$ into $-t_K, -t_{K-1}, \ldots, -t_1$ and the count time series from $n_1, n_2, \ldots, n_K$ into $n_K, n_{K-1}, \ldots, n_1$.

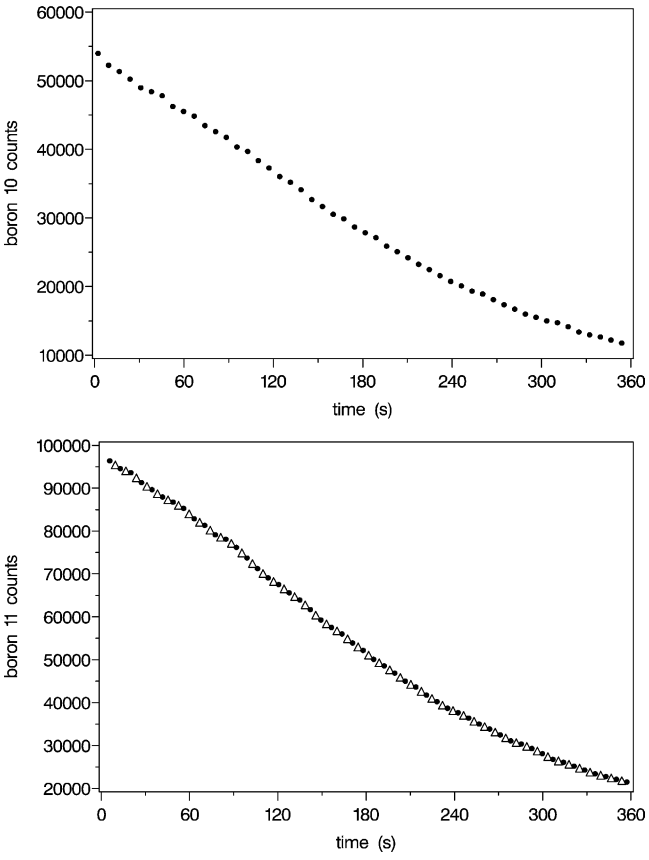

Fig. 2. Observed B10 counts (4 s time bins) (top). Observed B11 counts (2 s time bins) (bottom). We plot interpolated B11 values as triangles.

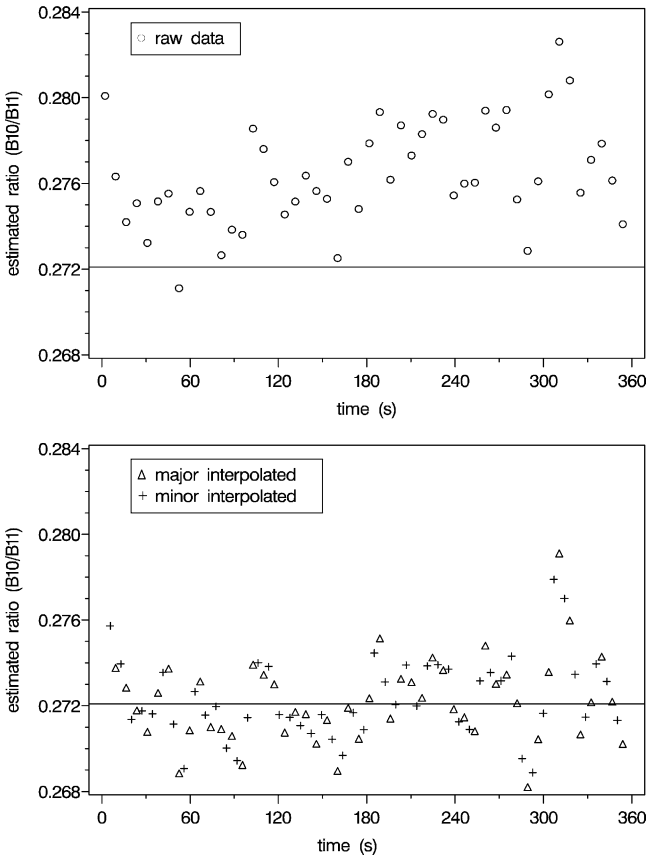

Fig. 3. Estimates of ratio of B10 to B11 isotopes computed from raw data (top). Estimates of ratio of B10 to B11 isotopes computed from both interpolation schemes (bottom). In both plots, we plot the average of the two interpolation estimates of the isotopic ratio as a reference line.

We list values of interpolation weights and interpolated count values computed from a subset of the data (Table 1) in Tables 2 and 3. Our subset consists of the first 15 cycles of data. For these 15 cycles, we estimate the ratio of B10 and B11 to be 0.27500 from the raw data. When the major counts are interpolated with respect to the minor counts, we estimate the isotopic ratio to be 0.27175 ± 0.00042. When the minor counts are interpolated with respect to the minor counts, we estimate the isotopic ratio to be 0.27189 ± 0.00041. The average of the estimates from the two interpolation schemes is 0.27182. The value of the goodness-of-fit statistic and associated *p*-value for testing the hypothesis that the true isotopic ratio is constant in time are 17.10 and 0.195.

Table 1
Observed B10 and B11 count data

k	$t_m(k)$	$m(k)$	$t_n(k)$	$n(k)$
1	2.323	53988	5.788	96378
2	9.473	52256	12.943	94555
3	16.639	51329	20.123	93598
4	23.839	50232	27.314	91306
5	31.014	48984	34.499	89640
6	38.205	48392	41.684	87935
7	45.380	47811	48.855	86763
8	52.550	46242	56.025	85283
9	59.720	45525	63.200	82870
10	66.906	44834	70.386	81326
11	74.081	43465	77.556	79122
12	81.251	42583	84.731	78091
13	88.432	41736	91.902	76205
14	95.602	40350	99.082	73738
15	102.772	39694	106.247	71249

$\Delta_m = 4$ s and $\Delta_n = 2$ s.

7. Simulation studies

7.1. Study 1: fixed number of bins

We next simulate Poisson count data where the count rate for the major isotope is similar to the observed experiment. The bins are the same as for the observed data (50 cycles with $\Delta_m = 4$ s and $\Delta_n = 2$ s for B10 and B11). We model the major count rate as

$$\lambda_n(t) = \sum_{k=0}^{4} a_k t^k, \tag{31}$$

where the polynomial model parameters are determined by fitting this model to the observed major count data shown in Fig. 2 by the method of weighted least squares. The agree-

Table 2
Interpolated B11 (major) data

k	$\alpha_n(k)$	$\beta_n(k)$	$\gamma_n(k)$	$\hat{n}(k)$
1	Undefined	Undefined	0.48498	Undefined
2	0.48498	0.51502	1.00026	95439
3	0.48524	0.51476	0.99801	94062
4	0.48324	0.51676	1.00180	92414
5	0.48504	0.51496	0.99916	90448
6	0.48420	0.51580	1.00039	88761
7	0.48459	0.51541	1.00007	87331
8	0.48466	0.51534	1.00036	86000
9	0.48502	0.51498	0.99926	84040
10	0.48427	0.51573	1.00038	82074
11	0.48466	0.51534	1.00036	80190
12	0.48502	0.51498	0.99888	78591
13	0.48389	0.51611	1.00079	77118
14	0.48468	0.51532	1.00032	74934
15	0.48500	0.51500	0.51500	72456

ment between the polynomial model and the observed major count data is very close. In order to avoid clutter, we do not plot the polynomial model prediction in the lower part of Fig. 2. In our simulation study, we assume that $\lambda_m(t) = r\lambda_n(t)$ where r varies. For each value of r, the expected number of total observed minor counts is approximately $5.5\ r \times 10^6$ and the expected number of total observed major counts is 2.7×10^6. For the lowest value of $r = 2.7 \times 10^{-6}$, the expected number of total minor counts, summed over all bins, is approximately 15.

In general, the average of the estimates from the two interpolation schemes is less biased than the estimate computed from the unaligned data or the estimate produced by either interpolation method (Table 4). The standard deviations of the estimates computed from each interpolation method, as well as their average, are well predicted by Eqs. (13) and (18) (Table 5). Finally, the rate at which we reject the hypothesis test with nominal size 0.05 is close to 0.05 except for smallest ratio (Table 6).

Based on the expected number of total major counts in this simulation experiment, Eq. (3) predicts a fractional bias of approximately 3.7×10^{-7}. This fractional bias is very small compared to the bias due to time bin misalignment. In a separate study, we equate the simulated count data to their expected value. For this noise-free data, the fractional bias of the average of the estimates computed from both interpolation methods is 1.5×10^{-7}. Thus, for cases where the major count rate has a shape like that in Fig. 2, as N tends to infinity, we expect that our interpolation method will introduce an asymptotic fractional bias of approximately 1.5×10^{-7}. In the event that a bias of this magnitude is considered to be scientifically significant, one might estimate it by a Monte Carlo method and correct the estimate accordingly. The fractional standard deviation of the $K - 1$ isotopic ratio estimates computed from the major–minor interpolation method for the noise-free data is 1×10^{-4}. For very high signal-to-noise ratio data like that we simulate, the hypothesis test would falsely detect systematic temporal variation at this level.

Table 3
Interpolated B10 (minor) data

k	$\alpha_m(k)$	$\beta_m(k)$	$\gamma_m(k)$	$\hat{m}(k)$
1	0.51538	0.48462	0.51538	53149
2	0.51577	0.48423	1.00038	51807
3	0.51611	0.48389	1.00034	50798
4	0.51568	0.48432	0.99957	49628
5	0.51537	0.48463	0.99969	48697
6	0.51512	0.48488	0.99976	48110
7	0.51534	0.48466	1.00022	47051
8	0.51534	0.48466	1.00000	45894
9	0.51573	0.48427	1.00038	45190
10	0.51498	0.48502	0.99926	44170
11	0.51534	0.48466	1.00036	43038
12	0.51539	0.48461	1.00005	42173
13	0.51604	0.48396	1.00065	41065
14	0.51464	0.48536	0.99861	40032
15	Undefined	Undefined	0.48536	Undefined

7.2. Study 2: variable number of bins

In our second study, we simulate Poisson count data corresponding to an experiment where a 100 s total observing time is divided into a variable number of time intervals. The widths of the minor isotope and major isotope intervals are the same. The spectrometer has two settings. In one, it measures minor isotopes. In the other, it measures major isotopes. The transition from one setting to the other does not occur instantly. In our simulation, we assume that there is a 0.2 s overhead time during the transition when no count data are collected. We assume that 0.2 s overhead time occurs at the beginning of each bin since the major and minor isotopes are measured in an alternating fashion. For instance, if there are 50 bins for counting major isotopes, and 50 bins for counting minor isotopes, the width of each bin is 1 s. Since data will not be collected during the initial 0.2 s of each bin, the fraction of the total 100 s observing time unavailable for recording data is 20%. Similarly, if there are 100 bins for counting major isotopes and 100 bins for counting minor isotopes, the fraction of the 100 s unavailable for recording data is 40%. In general, as the number of bins increases, the fraction of useful observing time relative to the full 100 s interval decreases.

For the kth interval for counting minor counts, we model the expected number of minor counts as

$$E(m(k)) = \int_{t_m(k)-\Delta_m/2+\delta}^{t_m(k)+\Delta_m/2} \lambda_m(t)\,\mathrm{d}t, \tag{32}$$

where $\delta = 0.2$ s and the width of the bin Δ_m depends on the number of bins. Similarly, for the kth major isotope interval, the expected number of major isotopes counts is

$$E(n(k)) = \int_{t_n(k)-\Delta_n/2+\delta}^{t_n(k)+\Delta_n/2} \lambda_n(t)\,\mathrm{d}t. \tag{33}$$

Table 4
Simulation study 1—fractional bias of estimate ($\times 10^4$)

True r	Unaligned	Major–minor alignment	Minor–major alignment	Average of both alignment estimates
1	134.95 ± 0.05	-0.27 ± 0.05	0.21 ± 0.05	-0.03 ± 0.05
0.27	135.01 ± 0.07	-0.21 ± 0.07	0.27 ± 0.07	0.03 ± 0.07
2.7E−03	135.88 ± 0.59	0.74 ± 0.59	1.13 ± 0.58	0.93 ± 0.59
2.7E−04	133.51 ± 1.85	-1.62 ± 1.86	-1.14 ± 1.83	-1.38 ± 1.84
2.7E−05	136.25 ± 5.85	3.31 ± 5.89	2.66 ± 5.81	2.99 ± 5.84
5.4E−06	141.57 ± 13.13	7.04 ± 13.18	6.93 ± 13.02	6.98 ± 13.08
2.7E−06	141.50 ± 18.71	2.31 ± 18.77	5.60 ± 18.55	3.96 ± 18.63

Assumed major isotope count rate based on Eq. (31) model for data shown in Fig. 2.

Table 5
Simulation study 1—fractional standard deviation of estimate ($\times 10^4$)

True r	Unaligned	Major–minor alignment	Minor–major alignment	Average of both alignment estimates
1	7.58	7.54 (7.49)	7.51 (7.45)	7.51
0.27	10.38	10.36 (10.34)	10.28 (10.25)	10.31
2.7E−03	83.30	83.63 (83.72)	82.64 (82.67)	83.01
2.7E−04	261.89	262.59 (264.06)	259.40 (260.74)	260.60
2.7E−05	827.96	833.31 (834.38)	822.00 (823.86)	826.45
5.4E−06	1856.47	1864.16 (1859.43)	1840.68 (1836.07)	1849.66
2.7E−06	2646.67	2653.87 (2616.58)	2622.89 (2584.22)	2634.46

Assumed major isotope count rate based on Eq. (31) model for data shown in Fig. 2. Mean predicted value in parentheses.

As before, we assume that the minor isotope is measured first. For time $0\,\text{s} < t < 100\,\text{s}$, we model the major count rate as

$$\lambda_n(t) = \lambda \exp\left(\frac{-t}{\tau}\right) \tag{34}$$

and the minor count rate as

$$\lambda_m(t) = r\lambda \exp\left(\frac{-t}{\tau}\right), \tag{35}$$

where $\tau = 100\,\text{s}/\ln(2)$ and $\lambda = 1000 \times \ln(2)\,\text{Hz}$ ($\approx 693\,\text{Hz}$) and $r = 0.1$. At $t = 100\,\text{s}$, the count rate is reduced by a factor of 2 compared to its value at $t = 0$.

In general, as the number of time bins K increases, the fractional bias of the isotopic ratio computed from the raw unaligned data decreases (Table 7). In all cases, the predicted and actual fractional standard deviation of estimates from either interpolation scheme are close (Table 8). However, as the number of bins increases, the signal-to-noise ratio of the data decreases since integrated overhead time depends on the total number of bins. The rejection rate of tests of nominal size 0.05 are close to their desired value for $10 \le K \le 100$ (Table 9). For the case of $K = 200$, the expected number of observed minor counts per bin varied from about 3.5 to 1.75 over the experiment. We attribute the degradation of the test performance to the fact that our chi-squared distribution assumption breaks down when applied to very low count data. In general, for cases where the rejection rate differs from 0.05, a bootstrap hypothesis test [7,12] might perform better than the one presented here.

Table 6
Simulation study 1—fractional bias of estimate ($\times 10^4$)

True r	Mean χ_r^2	Rejection rate
1	47.5681 ± 0.0731	0.0546
0.27	47.7875 ± 0.0700	0.0494
2.7E−03	48.0845 ± 0.0687	0.0485
2.7E−04	48.0289 ± 0.0698	0.0498
2.7E−05	47.9043 ± 0.0705	0.0521
5.4E−06	47.9502 ± 0.0754	0.0671
2.7E−06	47.8509 ± 0.0801	0.0763

Assumed major isotope count rate based on Eq. (31) model for data shown in Fig. 2. The hypothesis test has nominal size of 0.05. The 1-sigma sampling error for a rejection rate of 0.05 is 0.0015 since the number of trials is 20 000.

8. Extra variability

8.1. Systematic errors

In some experiments, the goodness-of-fit statistic (Eq. (26)) may be very large due to systematic errors even though the isotopic ratio is constant for all cycles. Below we outline a suggested strategy to quantify this systematic uncertainty. Verification of our suggested method is a topic for further study.

Our suggested method is based on the key assumptions that the true isotopic ratio for the ith cycle is a random variable $r(i) = r + \delta_i$, where $E(\delta_i) = 0$, $VAR(\delta_i) = \sigma_{\text{sys}}^2$, and the realizations of δ_i are independent. Based on the above assumptions, we modify our goodness-of-fit statistic, χ_r^2 (Eq. (26)) as follows

Table 7
Simulation study 2—fractional bias of estimate $\times 10^4$

Number of bins K	Unaligned	Major–minor alignment	Minor–major alignment	Average of both alignment estimates
5	717.96 ± 1.58	-23.23 ± 1.69	24.87 ± 1.55	0.82 ± 1.59
10	352.16 ± 1.55	-7.50 ± 1.60	4.53 ± 1.54	-1.49 ± 1.56
50	72.61 ± 1.68	2.76 ± 1.68	3.15 ± 1.67	2.95 ± 1.68
100	34.04 ± 1.91	-0.69 ± 1.92	-0.65 ± 1.91	-0.67 ± 1.91
150	25.30 ± 2.33	1.98 ± 2.34	2.05 ± 2.33	2.02 ± 2.34
200	14.43 ± 3.32	-2.62 ± 3.32	-2.70 ± 3.32	-2.66 ± 3.32

Exponential count rate based on Eq. (34).

Table 8
Simulation study 2

Number of bins K	Unaligned	Major–minor alignment	Minor–major alignment	Average of both alignment estimates
5	223.92	239.45 (240.06)	219.51 (220.10)	225.44
10	218.72	226.73 (227.40)	217.48 (218.37)	220.43
50	236.95	238.05 (237.42)	236.35 (235.58)	236.88
100	270.51	271.46 (272.47)	270.25 (271.41)	270.68
150	330.16	330.97 (333.10)	330.01 (332.24)	330.35
200	469.48	469.88 (470.49)	469.19 (469.58)	469.38

Exponential count rate based on Eq. (34). Fractional standard deviation of estimate $\times 10^4$. Mean predicted value in parentheses.

Table 9
Simulation study 2

Number of bins K	Mean χ_r^2	Rejection rate
5	2.9592 ± 0.0169	0.0459
10	7.9692 ± 0.0280	0.0489
50	47.9222 ± 0.0697	0.0494
100	97.7559 ± 0.0993	0.0487
150	148.0495 ± 0.1238	0.0538
200	198.0556 ± 0.1463	0.0602

Exponential count rate based on Eq. (34). The hypothesis test has nominal size of 0.05. The 1-sigma sampling error for a rejection rate of 0.05 is 0.0015 since the number of trials is 20 000.

$$\chi_r^2(\sigma_{\text{sys}}) = \sum_{k=2}^{K} \frac{(\hat{r}(k) - \hat{r})^2}{\widehat{\text{VAR}}(\hat{r}(k)) + \sigma_{\text{sys}}^2}. \tag{36}$$

We estimate σ_{sys} by requiring that $\chi_r^2(\sigma_{\text{sys}})$ equals its expected value under the null hypothesis that all variation is due to Poisson counting statistics and the isotopic ratio is the same for all cycles. Assuming that correlation effects due to interpolation are insignificant, for high count data sets where K is large enough, this expected value is approximately $K - 2$. For low count data sets where this approximation is not valid, a bootstrap resampling scheme similar to one in [7] might be a better approach to determine the expected value of the test statistic under the null hypothesis. Another strategy for determining σ_{sys} would be to require that $\int_{\chi_r^2(\sigma_{\text{sys}})}^{\infty} f(x)\,\mathrm{d}x$ equals 0.5, where $f(x)$ is the pdf for a chi-squared distribution with $K - 2$ degrees of freedom. A natural approximation for the variance of the estimate $\hat{r}$ due to both random variation and the additional systematic cycle to cycle variation estimated here is $\hat{\sigma}^2$ where

$$\hat{\sigma}^2 = \widehat{\text{VAR}}(\hat{r}) + \sigma_{\text{sys}}^2 \sum_{k=2}^{K} w_k^2, \tag{37}$$

where $w_k = \hat{n}(k)/\sum_{j=2}^{K} \hat{n}(j)$ and $\widehat{\text{VAR}}(\hat{r})$ is given by Eq. (13) or (18).

The validity of our suggested method is a subject for further research. There may be some subtle degree-of-freedom issues related to correlation induced by interpolation as well as the usual low count concerns (when the chi-square distribution assumption breaks down). Systematic errors that do not vary from cycle to cycle, e.g., mass bias effects, would not be quantified by our suggested approach.

8.2. Extra random variation

In this work, we have assumed that the observed count data for any cycle is a realization of a Poisson process. Hence, the mean and variance of the observed count data are assumed to be the same. If the variance of the measured count data is larger than the expected value, we expect that our formulas for the variance of isotopic ratio estimates (Eqs. (13), (18) and (28)) will underestimate the actual variances. Failing to account for extra random variability may systematically inflate the value of the goodness-of-fit statistic computed in Eq. (26), even if the isotopic ratio is constant over all cycles.

In principle, one could do experiments to check the equivalence of the mean and variance of observed count data for a sample where we knew the isotopic ratio was stable in time. Given this extra information, perhaps we could modify our variance approximations (Eqs. (14), (16), (18), (24), (25), (28), (29), (30)) and our goodness-of-fit statistic (Eq. (26)). Alternatively, we could estimate σ_{sys} using Eq. (36)

but interpret σ_{sys} differently. In this alternative interpretation, σ_{sys} would quantify the effect of unaccounted extra random variability in the data on our estimate of r according to Eq. (37). The validity of this approach is a subject for further study.

9. Summary

In this work, we corrected SIMS measurements of isotopic counts for drift by aligning the isotopic time series using two linear interpolation schemes. In one scheme, the major isotope time series is aligned with respect to the minor isotope time series. In the other scheme, the minor isotope time series is aligned with respect to the major isotope time series. We averaged the isotopic ratio estimates from both interpolation schemes. Our analytical formulas (Eqs. (13) and (18)) closely predicted the standard deviation of the isotopic ratio due to Poisson counting statistics variation computed in Monte Carlo simulation experiments. Since, on average, both Eqs. (13) and (18) predict nearly the same standard deviation of the mean estimate, we suggest that the user of our method report the larger of the two.

We presented an approximate hypothesis test procedure to detect and quantify possible temporal variation of the measured isotopic ratio. For most of the cases studied, the rejection rate of our test was close to the desired nominal value. The discrepancy was largest for cases where the number of minor counts was very low or the number of bins was very low (Tables 6 and 9). For cases where the hypothesis test (Eq. (26)) performance is inadequate, a bootstrap hypothesis test like that in [7] might be appropriate. We also provide a test data set (Table 1) from a subset of the boron data shown in Fig. 2, and list computed interpolation weights and interpolated count values in Tables 2 and 3. We offered guidance on how to quantify systematic errors that vary from cycle to cycle for cases where one knows that the isotopic ratio does not vary from cycle to cycle. We also suggested a method to quantify additional uncertainty in our estimate of the isotopic ratio for the case where the variability in the count data is greater than predicted by Poisson statistics. The validity of these two approaches is a subject for further study.

Here, we neglected dead time effects, mass bias effects and background contributions. Accounting for these effects in our estimation procedure and uncertainty analysis is a subject beyond the scope of this work. In this work, we presented a hypothesis test for temporal variation based on the $K-1$ ratio estimates from the major–minor interpolation scheme. It might be possible to develop a better hypothesis test based on the $2(K-1)$ ratio estimates from both interpolation schemes. There are other possible approaches for drift correction besides the one described here. For instance, one might simultaneously estimate the major count rate $\lambda_n(t)$ and the isotopic ratio r using a functional data analysis approach [13]. In such an approach, the continuously varying count rate might be modeled as a regression spline. Selecting the appropriate form and complexity of the regression spline would be a research project. In this work, we focused on the case where the total number of observed minor counts was greater than 0. Our methods are not intended for the cases where the total number of minor counts is 0. The 0 count case is a topic for further study.

Acknowledgement

We thank J. Splett of NIST for assistance with the preparation of this manuscript and helpful comments.

Appendix A. Propagation-of-error method

Suppose that x and y are independent random variables with expected values μ_x and μ_y and variances σ_x^2 and σ_y^2. Define the ratio $r = \mu_x/\mu_y$ and ratio estimate $\hat{r}$

$$\hat{r} = f(x, y) = \frac{x}{y}.$$

Following [7], we approximate f as a Taylor series expansion using its derivatives f_x, f_y and f_{xy}. We have

$$\begin{aligned}\hat{f}(x, y) = {} & f(\mu_x, \mu_y) + (x-\mu_x) f_x(\mu_x, \mu_y) \\ & + (y-\mu_y) f_y(\mu_x, \mu_y) + (x-\mu_x)(y-\mu_y) \\ & \times f_{xy}(\mu_x, \mu_y), \end{aligned} \tag{A.1}$$

where

$$f_x(\mu_x, \mu_y) = \frac{1}{\mu_y}$$

$$f_y(\mu_x, \mu_y) = \frac{-\mu_x}{\mu_y^2}$$

and

$$f_{xy}(\mu_x, \mu_y) = -\frac{1}{\mu_y^2}.$$

As noted in Section 3, we assume that x and y are independent and hence uncorrelated. If for some reason x and y were correlated, we would add a covariance term $2\,\mathrm{COV}(x, y) f_x(\mu_x, \mu_y) f_y(\mu_x, \mu_y)$ to the right hand side of Eq. (A.1).

We approximate the variance of $\hat{r}$ as

$$\widehat{\mathrm{VAR}}(\hat{r}) = E[\hat{f}(x, y) - f(\mu_x, \mu_y)]^2. \tag{A.2}$$

Hence

$$\widehat{\mathrm{VAR}}(\hat{r}) = \sigma_x^2 (f_x(\mu_x, \mu_y))^2 + \sigma_y^2 (f_y(\mu_x, \mu_y))^2 + \sigma_x^2 \sigma_y^2 (f_{xy}(\mu_x, \mu_y))^2. \quad \text{(A.3)}$$

Simplifying, we have that

$$\frac{\widehat{\mathrm{VAR}}(\hat{r})}{r^2} = \frac{\sigma_x^2}{\mu_x^2}\left(1 + \frac{\sigma_y^2}{\mu_y^2}\right) + \frac{\sigma_y^2}{\mu_y^2}. \quad \text{(A.4)}$$

Comments

One could include more terms in our Eq. (A.1) Taylor series expansion. For instance, in a complete second order expansion, we would add $\frac{1}{2}(y - \mu_y)^2 f_{yy}(\mu_x, \mu_y)$ to the right-hand side of Eq. (A.1), where $f_{yy}(\mu_x, \mu_y) = 2\mu_x/\mu_y^3$. However, the relative contribution due to this additional term to the variance approximation for $\hat{r}$ is negligible.

Appendix B. Codes

```
interpmajor = function(tm, m, tn, n, deltam, deltan){
# interpolate major count time with respect to minor count time series
# assume that the minor isotope is measured first
# tm,tn are midpoints of observing intervals for minor and major isotope counts
# m,n are observed minor and major isotope counts
# deltam, deltan are length of minor and major observing intervals
        K = length(m)
        KK = K - 1
        gamman = 1:K
        alphan = 1:K
        betan = 1:K
        nhat = 1:K
        Nhatsum = 0
        Msum = 0

        for(k in (2:K)){
               alphan[k] = (tn[k] - tm[k])/(tn[k] - tn[k - 1])
               betan[k] = (tm[k] - tn[k - 1])/(tn[k] - tn[k - 1])
               nhat[k] = alphan[k] * n[k - 1] + betan[k] * n[k]
               Nhatsum = Nhatsum + nhat[k]
               Msum = Msum + m[k]
       }
        for(k in (2:KK)){
               gamman[k] = alphan[k + 1] + betan[k]
       }
        gamman[1] = alphan[2]
        gamman[K] = betan[K]

        rhat = (Msum/deltam)/(Nhatsum/deltan)
        varMsum = Msum # variance approximation for Msum
        varNhatsum = sum(gamman^2 * n) # variance approximation for Nhatsum
        term1 = varMsum * (1 + varNhatsum/Nhatsum^2)
        term2 = ((deltam * rhat)/deltan)^2 * varNhatsum
        term3 = (deltan/(deltam * Nhatsum))^2
        unc2 = (term1 + term2) * term3
        unc = sqrt(unc2) # random 1-sigma uncertainty estimate

        out = 1:2
        out[1] = rhat # isotopic ratio estimate
        out[2] = unc # 1-sigma random uncertainty estimate
        out # return isotopic ratio and associated uncertainty
}
```

```
interpminor = function(tm, m, tn, n, deltam, deltan){
# interpolate minor count time series with respect to major count time series

       K = length(m)
       KK = K - 1
       alpham = 1:K
       betam = 1:K
       mhat = 1:K
       gammam = 1:K
       Mhatsum = 0
       Nsum = 0

       for(k in (1:KK)){
              alpham[k] = (tm[k + 1] - tn[k])/(tm[k + 1] - tm[k])
              betam[k] = (tn[k] - tm[k])/(tm[k + 1] - tm[k])
              mhat[k] = alpham[k] * m[k] + betam[k] * m[k + 1]
              Nsum = Nsum + n[k]
              Mhatsum = Mhatsum + mhat[k]
      }

       for(k in (2:KK)){
              gammam[k] = alpham[k] + betam[k - 1]
      }

       gammam[1] = alpham[1]
       gammam[K] = betam[K - 1]
       varNsum = Nsum
       varMhatsum = sum(gammam^2 * m)

       rhat = (Mhatsum/deltam)/(Nsum/deltan)

       term1 = varMhatsum * (1 + varNsum/Nsum^2)
       term2 = ((deltam * rhat)/deltan)^2 * varNsum
       term3 = (deltan/(deltam * Nsum))^2
       unc2 = (term1 + term2) * term3
       unc = sqrt(unc2)

       out = 1:2
       out[1] = rhat # isotopic ratio estimate
       out[2] = unc # 1-sigma random uncertainty estimate
       out # return isotopic ratio and associated uncertainty
}
```

```
temporaltest = function(tm, m, tn, n, deltam, deltan){
# test of hypothesis that the true isotopic ratio does not vary in time
       K = length(m)
       KK = K - 1
       gamman = 1:K
       alphan = 1:K
       betan = 1:K
       nhat = 1:K
       gof = 0
       Nhatsum = 0
       Msum = 0
       for(k in (2:K)){
              alphan[k] = (tn[k] - tm[k])/(tn[k] - tn[k - 1])
              betan[k] = (tm[k] - tn[k - 1])/(tn[k] - tn[k - 1])
              nhat[k] = alphan[k] * n[k - 1] + betan[k] * n[k]
              Nhatsum = Nhatsum + nhat[k]
              Msum = Msum + m[k]
      }
       for(k in (2:KK)){
              gamman[k] = alphan[k + 1] + betan[k]
      }
       gamman[1] = alphan[2]
       gamman[K] = betan[K]
       rhat = (Msum/deltam)/(Nhatsum/deltan) # isotopic ratio estimate
                                             # computed from pooled data
       for(k in (2:K)){
              est = (m[k]/deltam)/(nhat[k]/deltan) # get estimates of r
                                                   # for each cycle
              varnk = alphan[k]^2 * n[k - 1] + betan[k]^2 * n[k]
              varmk = ((deltam * rhat)/deltan) * nhat[k]
              term1 = varmk * (1 + varnk/nhat[k]^2)
              term2 = ((rhat * deltam)/deltan)^2 * varnk
              term3 = (deltan/(deltam * nhat[k]))^2
              varest = (term1 + term2) * term3
              gof = gof + (est - rhat)^2/varest
      }
       df = K - 2 # compute approximate degrees of freedom for gof
       pval = 1 - pchisq(gof, df) # compute approximate p-value
       out = 1:2
       out[1] = gof
       out[2] = pval
       out # return goodness-of-fit statistic and p-value
}
```

References

[1] T.R. Ireland, Advances in Analytical Geochemistry, vol. 2, JAI Press, Greenwich, 1995.
[2] D. Donohue, IAEA Bull. 44 (2) (2002).
[3] G. Tamborini, M. Betti, V. Forcina, T. Hiernaut, B. Giovannone, L. Koch, Spectrochim. Acta Part B 53 (1998) 1289–1302.
[4] P.R. Danesi, A. Markowicz, E. Chinea-Cano, W. Burkart, B. Salbu, D. Donohue, F. Ruedenauer, M. Hedberg, S. Vogt, P. Zahradnik, A. Ciurapinski, J. Environ. Radioactivity 64 (2–3) (2003) 143–154.
[5] D.S. Simons, J. Trace Microprobe Tech. 4 (1986) 185–195.
[6] D.S. Simons, in: A. Benninghoven, K.T.F. Jannsen, J. Tumper, J.W. Werner (Eds.), Proceedings of the 8th International Conference on Secondary Ion Mass Spectrometry (SIMS VIII), Wiley, New York, 1991, pp. 714–718.
[7] K.J. Coakley, D.S. Simons, Chemometrics Intelligent Lab. Syst. 41 (1998) 209–220.
[8] J.M. Hayes, D.A. Schoeller, Anal. Chem. 49 (1977) 306–311.
[9] W. Feller, On Probability Problems in the Theory of Counters Studies and Essays, Interscience, 1948.
[10] A.M. Wood, F.A. Graybill, D.C. Boes, In Introduction to the Theory of Statistics, third ed., McGraw-Hill, New York, 1974.
[11] The R Project for Statistical Computing, http://www.r-project.org/.
[12] B. Efron, R.J. Tibshirani, An Introduction to the Bootstrap, Chapman & Hall, New York, 1993.
[13] J.O. Ramsey, B.W. Silverman, Functional Data Analysis, Springer, New York, 1997.